

Study on Wear, Cutting and Chipping Behaviors of Hydrogenated Nitrile Butadiene Rubber Reinforced by Carbon Black and *In-Situ* Prepared Zinc Dimethacrylate

Zheng Wei,¹ Yonglai Lu,^{1,2} Yang Meng,¹ Liqun Zhang^{1,2}

¹Key Laboratory of Beijing City for Preparation and Processing of Novel Polymer Materials, Beijing University of Chemical Technology, Beijing 100029, China

²Key Laboratory for Nanomaterials of Ministry of Education, Beijing University of Chemical Technology, Beijing 100029, China

Received 28 March 2011; accepted 18 August 2011

DOI 10.1002/app.35486

Published online 5 December 2011 in Wiley Online Library (wileyonlinelibrary.com).

ABSTRACT: In this study, the wear (Akron and DIN) and the cutting and chipping (C&C) behaviors of hydrogenated nitrile butadiene rubber (HNBR) reinforced by carbon black (N115) and *in-situ* prepared zinc dimethacrylate (ZDMA) were investigated. It was validated that ZDMA was more effective than N115 to enhance the wear and C&C resistance of HNBR composites. The Akron wear resistance of the HNBR/N115 composites increased with the content of ZDMA, and the Schallamach ridges observed on the abraded surfaces became less and less clear. With increasing content of ZDMA, the failure mode of the DIN abraded surface underwent the transition from craters to Schallamach ridges, and finally to scratches. The

HNBR/N115 composite reinforced by 10 phr ZDMA had the best DIN wear resistance when Schallamach ridges were the dominant failure mode. The use of 30 phr ZDMA can dramatically enhance the C&C resistance of the HNBR/N115 composites. The C&C resistance was suggested to be related to both the variation of the morphology of the C&C ridges and the direction of crack propagation as a function of the content of ZDMA. © 2011 Wiley Periodicals, Inc. *J Appl Polym Sci* 124: 4564–4571, 2012

Key words: nanocomposites; reinforcement; rubber; HNBR; ZDMA

INTRODUCTION

In recent years, hydrogenated nitrile butadiene rubber (HNBR) has become a fast growing raw material used in specialized industrial applications such as oil well packers, hoses, power transmission, timing belt, and tank track pads because of its excellent aging resistance to oil and hot-air, high static and dynamic mechanical strength, and wear resistance, especially at elevated temperatures.^{1–3} The dramatic reinforcement effect of HNBR by zinc dimethacrylate (ZDMA) was discovered in the late 1980s, which attracted the significant interest of researchers.^{4–13} During the peroxide curing process, the ZDMA dispersed in the HNBR matrix can take part in *in-situ*

polymerization and phase separate into nano-sized reinforcing domains.

The wear behavior of rubber materials is a complex phenomenon and involves a combination of several different mechanisms, the most dominant of which are adhesive wear and abrasive wear.^{14–19} The two dominant wear mechanisms can be clearly distinguished by the wear patterns observed on the abraded surface of rubber materials. Schallamach ridges, the best studied wear pattern in the last 60 years, are mainly caused by adhesive wear. The ridges were generated from the strong interfacial adhesion motion on the abraded surface when soft rubber slides over a smooth hard counterface.^{14–19} Other wear patterns, such as scratches and craters, are mainly caused by abrasive wear. These patterns were generated mainly by a cutting-rupture action of sharp angular asperities on the sliding counterface or as third bodies (particles).^{16,19}

In order to predict the lifetimes and increase the life expectancy of rubber components, especially for expensive rubbers such as HNBR, a good understanding of the failure mechanisms of wear is extremely essential. However, the wear behavior of the rubber based on a single experimental wear test cannot be directly correlated to the behavior of the rubber in practical applications, so it is necessary to

Correspondence to: L. Zhang (zhanglq@mail.buct.edu.cn).

Contract grant sponsor: National Science Fund for Distinguished Young Scholars; contract grant number: 50725310.

Contract grant sponsor: Cheung-kong Scholars Program of Ministry of Education.

Contract grant sponsor: National High Technology Research and the Development Program of China; contract grant number: 2009AA03Z338.

TABLE I
Formulations of HNBR/N115/ZDMA and HNBR/N115 Compounds

Ingredients	HNBR/N115/ZDMA (phr)				HNBR/N115 (phr)				
	A1	A2	A3	A4	B1	B2	B3	B4	B5
HNBR	100	100	100	100	100	100	100	100	100
N115	20	20	20	20	20	30	40	50	60
ZDMA/(ZnO/MAA)	10	20	30	40	–	–	–	–	–
TOTM	2	2	2	2	2	2	2	2	2
AO-445	2	2	2	2	2	2	2	2	2
DCP	4	4	4	4	4	4	4	4	4
TAIC	1	1	1	1	1	1	1	1	1

evaluate the wear behavior in different types of wear test. Although several studies have reported the excellent wear resistance of HNBR,^{20–24} the wear behavior in different types of wear test (with different dominant mechanisms) of HNBR composite reinforced by *in-situ* prepared ZDMA was seldom reported and studied, especially the correlation between the morphology of the abraded surface and the wear performance of the composite.

In recent years, the cutting and chipping (C&C) test was developed as a novel and quick laboratory measurement to evaluate the resistance of rubber materials to hard rocks or other sharp asperities, and a variety of studies on the C&C test reported a good correlation between laboratory test and actual service performance.^{25–29} However, there have been almost no relative studies on the C&C resistance of HNBR composites, especially ZDMA reinforced HNBR composite.

The motivation of this work was an attempt to identify promising combinations of HNBR and the reinforcing material ZDMA by laboratory techniques to comprehensively evaluate both the wear and C&C properties and build the relationships between the properties and the mechanisms. Moreover, this work may also help to optimize material selection for HNBR composites intended for specific applications.

EXPERIMENTAL

Materials

The matrix rubber used in this work was HNBR [Zetpol 2010L (bound nitrile 36%, 4% double bond), Zeon Chemical Co., Japan]. The fillers used were carbon black [N115 (density 345 kg/m³, dibutyl phthalate absorption 113 cm³/100 g, iodine number 160 g/kg), Degussa Carbon Black Co., Ltd., Tianjin, China], zinc oxide [ZnO (industrial grade), Yachang Chemical Co., Ltd., Tianjin, China], and dimethacrylic acid [MAA (purity 98%), Yili Fine Chemical Co., Ltd., Beijing, China]. The peroxide crosslinking agent used was dicumyl peroxide [DCP (purity 99.8%), AkzoNoble Chemicals Co., Ltd., Ningbo,

China] and the co-curing agent used was triallyl isocyanurate [TAIC (purity 95%), WahSing Chemical Co., Ltd., Jiangsu, China]. The plasticizer trioctyl trimellitate [TOTM (density 0.988, boiling point 258°C), Huayi Plastics Technical Co., Ltd., Jiangsu, China] and antioxidant [AO-445 (purity 69%), Actmix Polymer Co., Ltd., Ningbo, China] were used as received.

Formulations and preparation

All the compounds described in Table I were mixed on a 6-inch two roll mill. Additionally, in order to achieve excellent dispersion of ZDMA for outstanding reinforcement effect, the ZDMA for HNBR/N115/ZDMA compounds shown in Table I (A1–A4) were prepared *in-situ* through the neutralization of ZnO/MAA molar ratio of 1 : 2 during the mixing process.¹² For HNBR/N115/ZDMA compounds, ZnO was added first in HNBR and mixed for 5 min, then MAA was added slowly while mixing, and the period was 10 min. After MAA was added, another 5 min mixing was followed, and carbon black and other agents were added at last. The cured composite was prepared in a compression mold under 15 MPa at 170°C for the optimum curing time T_{90} as determined by a disc oscillating rheometer (P355B2, Huanfeng Chemical Technology and Experimental Machine Plant, Beijing, China).

Characterization

Transmission electron microscopy (TEM) observations of the HNBR/ZDMA compound and vulcanizate were performed on a Hitachi H-800 model (Tokyo, Japan). The thin sections for TEM observations were cut by a microtome under –100°C and collected on copper grids. The morphology was determined by using an accelerating voltage of 200 kV.

Scanning electron microscopy (SEM) observations of the tested surfaces of the samples after wear and C&C tests were performed on a Hitachi S-4700 model (Tokyo, Japan). The tested surfaces were cut from the samples and coated with platinum in an

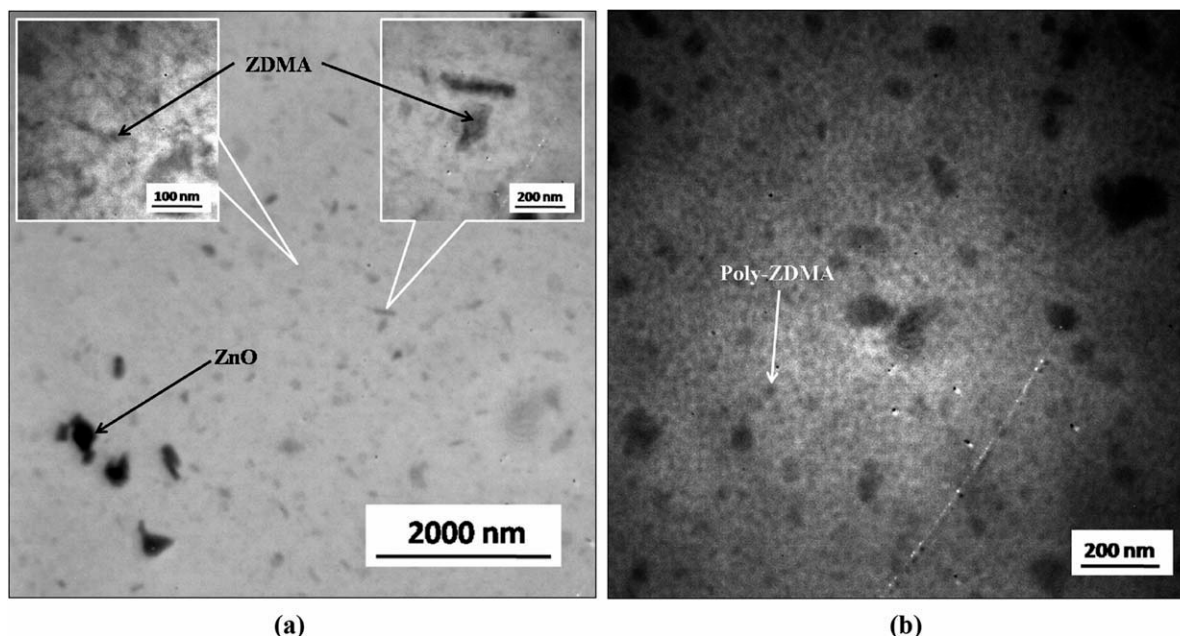


Figure 1 TEM images of HNBR/ZDMA (a) compound and (b) vulcanizate.

SPI sputter coater. The morphology was determined by using an accelerating voltage of 20 kV.

Tensile tests were performed on a SANS CTM-4104 model tensile tester (Shenzhen, China) at constant temperature and humidity according to Chinese Standards GB/T528-1998 and GB/T529-1999.³⁰ Tensile tests were carried out at a speed of 500 mm/min. Five specimens were tested for each recipe to obtain the mean and standard deviation of the measurements for the sample.

The Akron wear test was carried out on an Akron abrader MZ-4061 model (Mingzhu Experimental Machine Plant, Jiangdu, China). The slip angle was 15°, and the rotational speed of the abrader was 76 RPM under a loading of 26.7 N. All the specimens were pre-abraded for 1000 revolutions before testing, and at least three specimens were tested to obtain the mean value of the Akron volume loss for each recipe.

The DIN wear test was carried out on a DIN abrader GM-1 model (Xinzhenwei Experimental Machine Plant, Jiangdu, China). The cylindrical specimens (16 mm in diameter and 12 mm in thickness) were abraded across a test emery paper of grade 60 under a constant force (10 N) and at a constant speed (0.32 m/s) of the roller. At least six specimens per recipe were tested to obtain the mean value of the DIN volume loss.

The C&C test was performed on a Goodrich C&C tester. The rotational speed was 720 RPM, and the frequency was 2 Hz. The volume loss of the specimens was determined under a test time of 20 min. At least three specimens per recipe were performed to obtain the mean value of the C&C volume loss.

RESULTS AND DISCUSSION

Morphological analyses

The TEM images of HNBR/ZDMA before and after curing are shown in Figure 1. For a clear evaluation of the dispersion level of the *in-situ* prepared ZDMA and the generated poly-ZDMA particles, the specimen used for TEM analysis was not mixed with carbon black. It can be observed from Figure 1(a) that almost all the *in-situ* prepared ZDMA particles were dispersed on the nano-scale level in the HNBR matrix before curing. After curing, there were significant amounts of nano-sized poly-ZDMA ionic clusters generated, as shown in Figure 1(b).

Mechanical properties

Table II shows the mechanical properties of HNBR/N115/ZDMA composites as a function of the content of ZDMA. With the increase of the content of ZDMA, most mechanical properties (especially the tear strength and modulus) of the composites dramatically increase because there were strong interactions (including chemical graft and physical adsorption) between the HNBR matrix and *in-situ* generated poly-ZDMA ionic clusters.^{4–9} However, the elongation at break decreases significantly with the increase of the content of ZDMA.

Wear behavior

Figure 2 depicts the variation of Akron and DIN wear volume losses of the HNBR composites with the content of reinforcing fillers. It can be clearly

TABLE II
Mechanical Properties of HNBR/N115/ZDMA Composites as a Function of ZDMA Content

Properties	B1	A1	A2	A3	A4
Tensile strength (MPa)	22.0 ± 1.4	27.9 ± 0.5	31.4 ± 1.1	36.7 ± 0.9	38.0 ± 0.5
Elongation at break (%)	530 ± 9	482 ± 5	469 ± 6	384 ± 7	294 ± 2
Tear strength (kN/m)	32.2 ± 1.0	45.3 ± 0.3	64.2 ± 2.0	77.2 ± 0.9	79.1 ± 1.0
Modulus at 100% (MPa)	1.32 ± 0.02	2.31 ± 0.09	4.32 ± 0.03	6.53 ± 0.21	9.94 ± 0.15
Modulus at 300% (MPa)	6.82 ± 0.22	14.33 ± 1.42	20.93 ± 0.60	25.24 ± 0.81	–
Shore A hardness (°)	61 ± 2	74 ± 1	80 ± 1	87 ± 2	89 ± 1
Permanent set (%)	4 ± 1	20 ± 1	20 ± 2	20 ± 2	20 ± 2

seen that ZDMA was much more effective than N115 to enhance the wear resistance of the HNBR composites. For the HNBR/N115/ZDMA composite, the Akron wear resistance increases with the content of ZDMA. However, the best DIN wear resistance was achieved at a ZDMA content of 10 phr, and the DIN volume loss increases with the further increases in the content of ZDMA.

Figure 3 shows the SEM images of the abraded surfaces of HNBR/N115/ZDMA composites reinforced by different contents of ZDMA after the Akron wear test. Schallmach ridges can be observed on the abraded surfaces; however, the ridges became less and less clear with increasing content of ZDMA. For rubber materials, Schallmach ridges can be brought on by wear on a hard abrader surface with blunt or sandpaper asperities.¹⁹ The stick-slip motion (also called “elastic deformation wear”) was the dominant mechanism to generate the ridges, and the volume losses of the rubber composites were mainly due to tear-tensile rupture failure at the root of the ridges.^{17–19,31,32} In this work, we found that with the increase of the content of ZDMA, there were reductions not only in the adhesion friction,²² but also in the capacity of deformation because of the increasing modulus (as shown in

Table II). As a result, the volume loss decreased and the ridges became less distinct with the increase of the content of ZDMA.

The SEM images of the DIN abraded surfaces of HNBR/N115/ZDMA composites with different contents of ZDMA are shown in Figure 4. It can be seen from Figure 4(a) that there are a large number of craters on the abraded surface of the HNBR/N115 (100/20) composite with no ZDMA. With the increase of the content of ZDMA, Schallmach ridges appear on the abraded surface; however, with further increases in the content of ZDMA, these ridges become less distinct and are replaced by scratches that are more continuous and parallel to the direction of sliding since the content of ZDMA was up to 20 phr.

Figure 5 shows a schematic sketch about the variation of wear patterns on an abraded surface with the content of ZDMA. Because of the low strength of the pure HNBR/N115 composite, the surface of the composite was easily fractured by the sharp asperities on the sandpapers, leaving a large number of craters. With the increase of the content of ZDMA, the surface of the specimen can no longer be easily fractured as a result of the dramatic increase in both tensile and tear strength, and Schallmach ridges

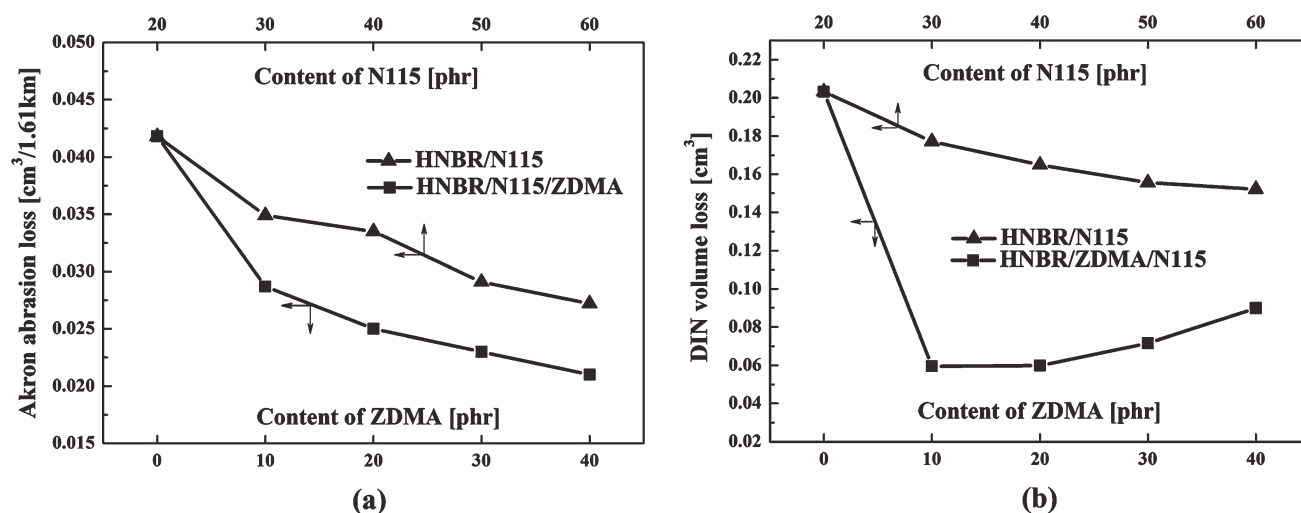


Figure 2 Variation of wear resistance of HNBR/N115 and HNBR/N115/ZDMA composites with content of reinforcing fillers: (a) Akron abrasion and (b) DIN abrasion.

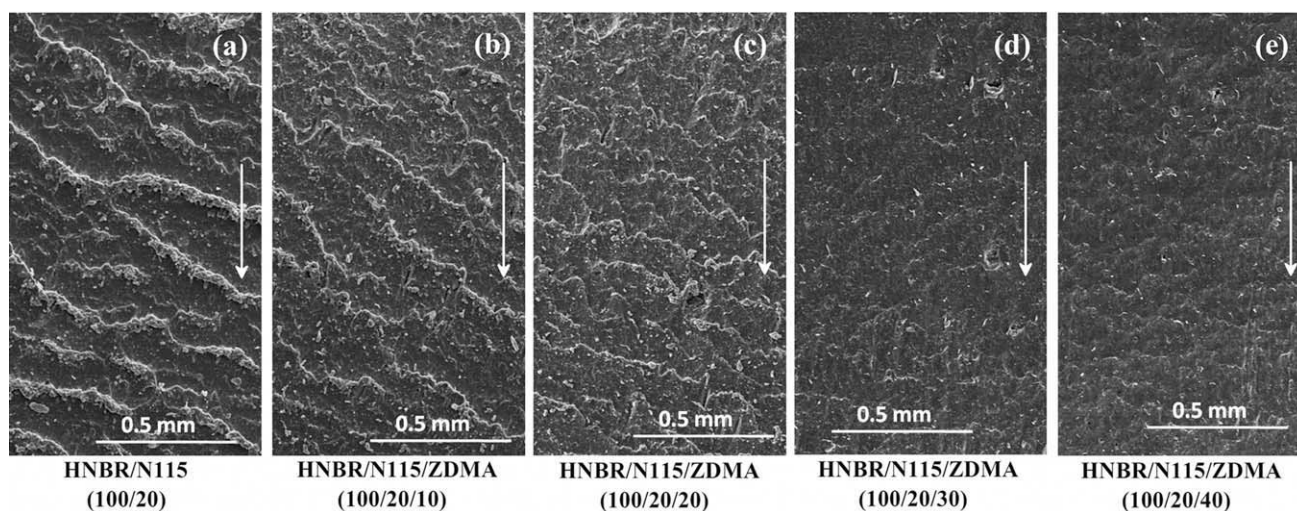


Figure 3 SEM images taken of abraded surfaces after Akron abrasion test: (a) HNBR/N115 (100/20) composite (B1); (b)–(e) HNBR/N115 (100/20) composites mixed with 10, 20, 30, 40 phr ZDMA respectively (A1–A4). The sliding direction is indicated by arrows.

appeared on the abraded surface. However, with the further increases in the content of ZDMA (≥ 20 phr), the wear mechanism of the HNBR/N115/ZDMA composite switched from “elastic deformation wear” to “plastic deformation wear” as a result of the marked increase of the modulus and decrease of the elongation at break. In this case, the real area of contact at the tip of the asperity is small, so the stress applied by the tip of the asperity may be so large that the abraded surfaces are detached from the bulk of the sample.¹⁴ Therefore, the dramatic increase of the DIN wear volume loss was supposedly related to the appearance of scratches that were actually brittle fractures caused by the abrasive and cutting wear by the sharp asperities on the surface of sandpaper.

Cutting and chipping resistance

Figure 6 shows the variation of C&C volume loss of the HNBR composites with the content of reinforcing fillers. It can be seen that the C&C resistance of the HNBR composites increases with the content of reinforcing fillers up to an N115 content of about 50 phr or a ZDMA content of about 30 phr. Besides, as in the case of wear resistance, ZDMA was also more effective than N115 to endow HNBR with C&C resistance.

The optical images of the test specimens with different contents of ZDMA are shown in Figure 7. Many ridges can be observed on the tested surfaces of the HNBR/N115/ZDMA composites. In this work, two parameters, d and h , were defined to

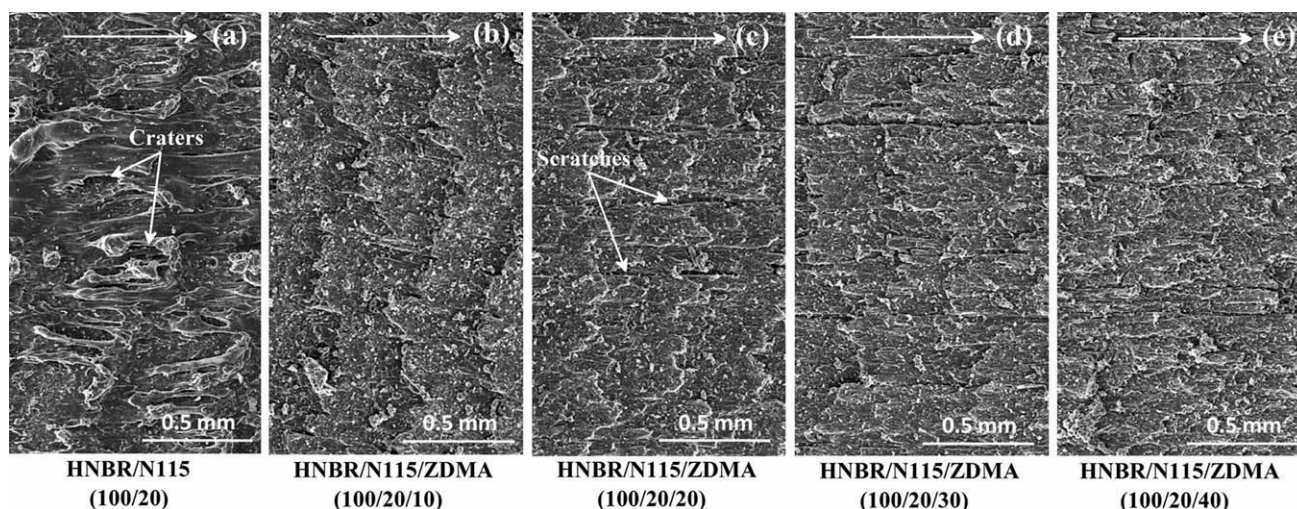


Figure 4 SEM images taken of abraded surface after DIN abrasion test: (a) HNBR/N115 (100/20) composite (B1); (b)–(e) HNBR/N115 (100/20) composites mixed with 10, 20, 30, 40 phr ZDMA, respectively (A1–A4). The sliding direction is indicated by arrows.

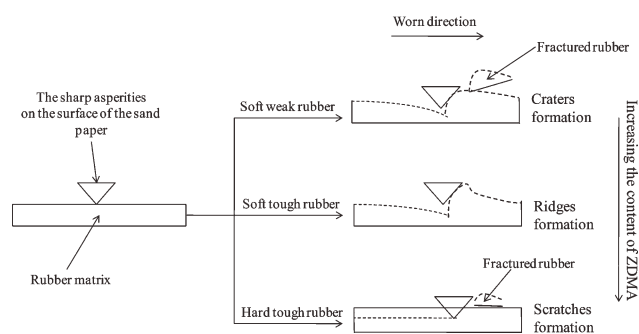


Figure 5 Schematic sketch about formation of wear patterns (craters, ridges, and scratches) on DIN abraded surface.

describe the C&C ridges. As illustrated in Figure 7(b), the parameter d is the width of a C&C ridge, and h is the distance between the two neighboring C&C ridges. With the increase of the content of ZDMA, there were a remarkable increase of d and a decrease of h ; especially, h was difficult to measure when ZDMA exceeded 40 phr.

Figure 8 shows the SEM images of the test surfaces after C&C testing. For the HNBR/N115 composite without ZDMA, as shown in Figure 8(a), severe C&C happened on the test surface because of the poor capacity of the composite to branch the large cracks. So ridges could not be observed on the test surface of the specimen. With the increase of the content of ZDMA, the number of cracks markedly increased because the generated nano-dispersed poly-ZDMA could dramatically enhance the capacity of the composite to branch the large cracks and convert part of the mechanical energy into surface energy. Furthermore, many cracks that extended vertically to the test surface can be clearly seen in Figure 8(f), presumably because the main direction of crack extension during the C&C process dramati-

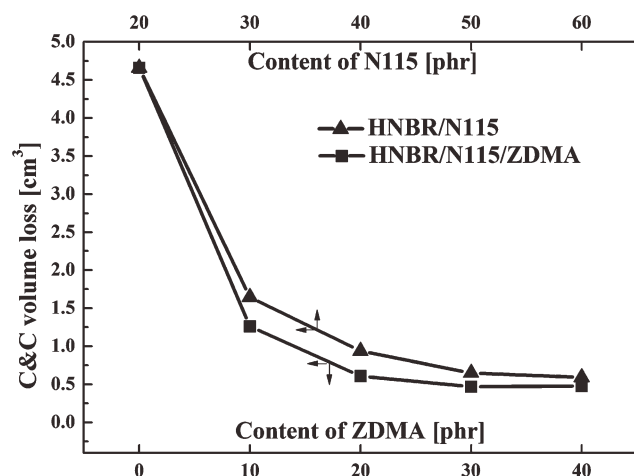


Figure 6 Variation of C&C volume loss of HNBR/N115 and HNBR/N115/ZDMA composites with the content of reinforcing fillers.

cally changed as the content of ZDMA reached 40 phr.

Figure 9 shows a schematic sketch of the variation of the deformation and crack initiation types during the C&C process with increasing content of ZDMA. As illustrated in Figure 9, the composites with low contents of ZDMA can undergo a larger deformation than those with high contents of ZDMA during C&C, because of the increase of the modulus and the decrease of the elongation at break with the increase of the content of ZDMA. Therefore, it was supposed to be an important reason for the increase of d with the increase in content of ZDMA. Furthermore, because of the decrease of the deformation ability of the composite, the direction of the crack initiated during the C&C process also varied from horizontal to vertical with the increase of the content of ZDMA, as shown in Figure 9(b), finally resulting in the decrease of h .

The positive effect of ZDMA on C&C resistance was the result of the special reinforcement structures of poly-ZDMA ionic clusters. Compared with the widely used reinforcement filler, carbon black, poly-ZDMA has much stronger interactions such as physical adsorption and chemical grafting between the poly-ZDMA ionic clusters and the rubber matrix. Therefore, the rubber matrix reinforced by ZDMA had much better mechanical properties and higher performance to prevent crack propagation than that reinforced by carbon black.⁵⁻⁹ Moreover, the ionic bond between Zn^{2+} and COO^- is a weak bond that can be easily destroyed and quickly recovered under large deformations or forces. Therefore, during the C&C process, the destruction and recovery of the

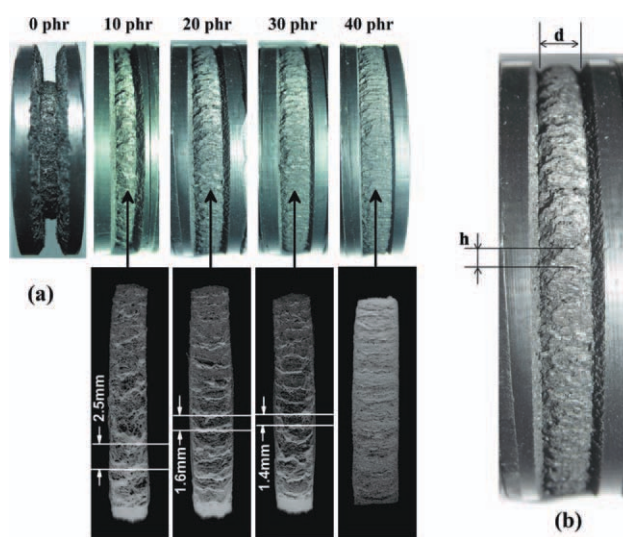


Figure 7 (a) Optical images of specimens with different content of ZDMA after C&C test; (b) illustration of parameters describing C&C ridges. [Color figure can be viewed in the online issue, which is available at wileyonlinelibrary.com.]

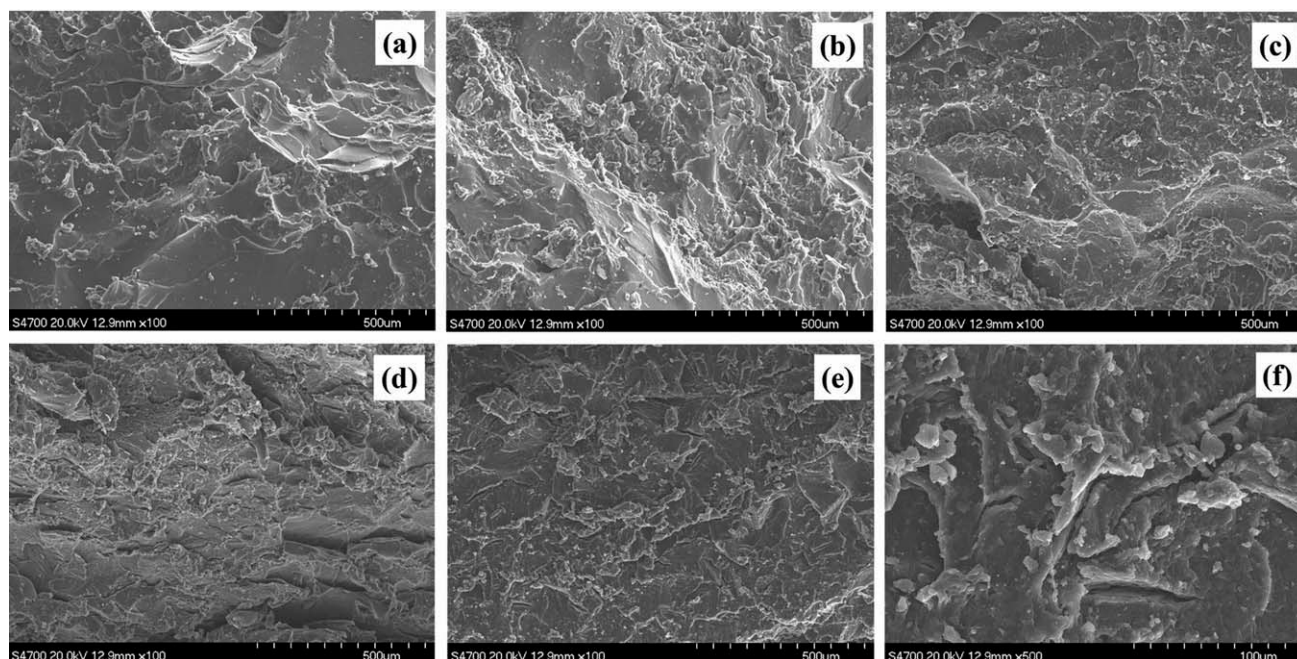


Figure 8 SEM images of C&C surfaces of HNBR/N115/ZDMA composites with different contents of ZDMA (B1, A1–A4): (a) 0 phr, (b) 10 phr, (c) 20 phr, (d) 30 phr, (e) and (f) 40 phr.

ionic cluster structure can result in high hysteresis and heat build-up, both leading to good C&C resistance.²⁵ However, the increase in hysteresis and heat build-up with the content of ZDMA had no effect on the C&C resistance at ZDMA contents above 30 phr, as explained by the following two reasons: (1) the capability of deformation and the rebound (as shown in Fig. 10) for HNBR/N115/ZDMA composites decreased significantly at high contents of ZDMA (because of the marked increase of the modulus and hardness), resulting in the applied external mechanical energy transforming into the new sur-

face energy induced by crack propagation; (2) the conversion rate of metal salts of unsaturated carboxylic acids was relatively low at high loadings,¹³ so the cracks can be easily initiated at the locations of the residual micro-sized ZDMA particles.

CONCLUSIONS

In this work, HNBR/N115 composites reinforced by *in-situ* prepared ZDMA were prepared. ZDMA was more effective than N115 to enhance both the wear and C&C resistance of the HNBR composites. The

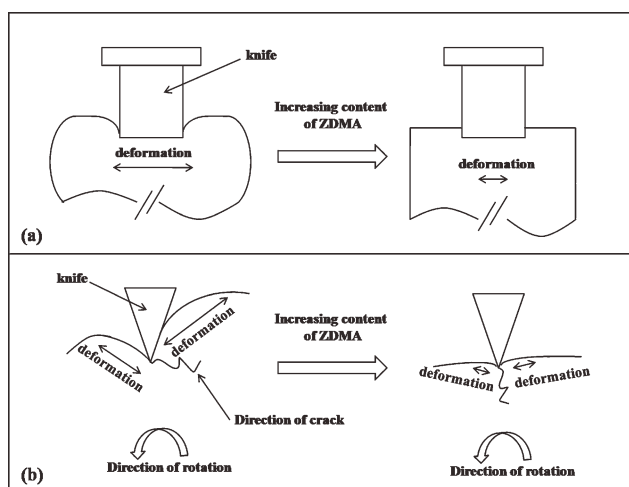


Figure 9 Schematic sketch of variation of deformation and crack initiation types with increasing content of ZDMA during C&C process.

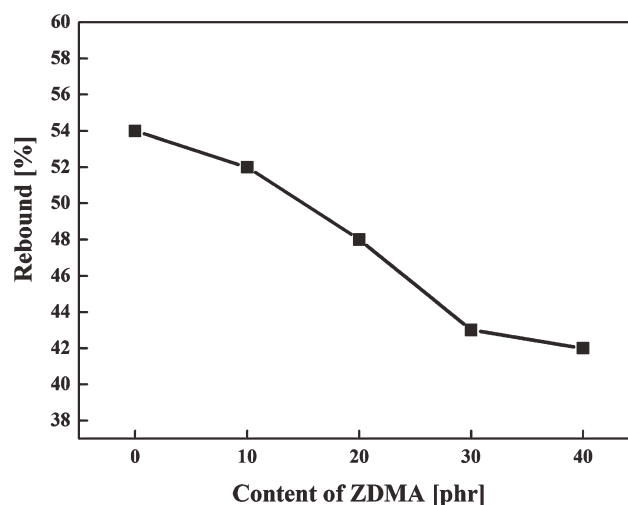


Figure 10 Rebound properties of HNBR/N115/ZDMA composites as a function of ZDMA content.

wear and C&C behavior of the HNBR/N115/ZDMA composites strongly depended on both the content of the ZDMA and the type of wear. The results can be summarized as follows:

1. The Akron wear resistance of HNBR/N115/ZDMA composite increased with the increase of the content of ZDMA. Schallamach ridges can be observed on the abraded surfaces, but the ridges become less clearly defined with the increase of the content of ZDMA.
2. The best DIN wear resistance of HNBR/N115/ZDMA composite was achieved at a ZDMA content of 10 phr, and the DIN volume loss increased with further increases in the content of ZDMA. With the increase of the content of ZDMA, the failure mode of the abraded surface changed from craters (neat HNBR/N115) to Schallamach ridges and finally to scratches; the wear mechanism changed from elastic deformation failure to plastic deformation failure.
3. The C&C resistance of HNBR/N115/ZDMA increased with increasing content of ZDMA, until the volume loss reached a certain value since ZDMA was up to 30 phr. The C&C resistance of HNBR/N115/ZDMA was supposed to be related to the variation of the morphology of the C&C ridges and the direction of crack propagation with the content of ZDMA.

References

1. Wrana, C.; Reinartz, K.; Winkelbach, H. R. *Macromol Mater Eng* 2001, 286, 657.
2. Nakagawa, T. *J Elastom Plast* 1992, 24, 240.
3. Tocuchet, P.; Rodriguez, G.; Gatzka, P. E.; Butler, D. P.; Crawford, D.; Teets, A. R.; Feuer, H. O.; Flanagan, D. P. U.S. Pat. 4,843,114 (1989).
4. Klingender, R. C.; Oyama, M.; Satio, Y. *Rubber World* 1990, 202, 26.
5. Saito, Y.; Nishimura, K.; Asada, M.; Toyoda, A. *J Jpn Rubber Soc* 1994, 67, 867.
6. Nomura, A.; Takano, J.; Toyoda, A.; Saito, T. *J Jpn Rubber Soc* 1993, 66, 830.
7. Hamed, G. R. *Rubber Chem Technol* 2007, 80, 534.
8. Lu, Y. L.; Liu, L.; Yang, C.; Tian, M.; Zhang, L. Q. *Eur Polym J* 2005, 41, 577.
9. Lu, Y. L.; Liu, L.; Tian, M.; Geng, H. P.; Zhang, L. Q. *Eur Polym J* 2005, 41, 589.
10. Ikeda, T.; Yamada, B. *Polym Int* 1999, 48, 367.
11. Ikeda, T.; Yamada, B.; Tsuji, M.; Sakurai, S. *Polym Int* 1999, 48, 446.
12. Wang, Y. H.; Peng, Z. L.; Zhang, Y.; Zhang, Y. X. *China Rubber Synth Ind* 2005, 28, 205.
13. Yin, D. H.; Zhang, Y.; Peng, Z. L.; Zhang, Y. X. *Eur Polym J* 2003, 39, 99.
14. Grosch, K. A. *Proc R Soc London A* 1963, 274, 21.
15. Schallamach, A. *Wear* 1971, 17, 301.
16. Medalia, A. I. *Kautschuk Gummi Kunststoffe* 1994, 47, 364.
17. Veith, A. G. *Rubber Chem Technol* 1992, 65, 601.
18. Bhowmick, A. K. *Rubber Chem Technol* 1982, 55, 1055.
19. Petitet, G.; Loubet, J.-L.; Zahouani, H.; Mazuyer, D. *Rubber Chem Technol* 2005, 78, 312.
20. Medalia, A. I.; Alesi, A. L.; Mead, J. L. *Rubber Chem Technol* 1992, 65, 154.
21. Thavamani, P.; Bhowmick, A. K. *Rubber Chem Technol* 1992, 65, 31.
22. Thavamani, P.; Bhowmick, A. K. *J Mater Sci* 1993, 28, 1351.
23. Xu, D.; Karger-Kocsis, J.; Apostolov, A. A. *Eur Polym J* 2009, 45, 1270.
24. Karger-Kocsis, J.; Felhös, D.; Xu, D. *Wear* 2010, 268, 464.
25. Beatty, J. R.; Miksch, B. J. *Rubber Chem Technol* 1982, 55, 1531.
26. Nan, C. W.; Jo, B. W.; Kaang, S. Y. *J Appl Polym Sci* 1998, 68, 1537.
27. Schwarz, D. L.; Askea, D. W. *Rubber World* 2003, 215, 28.
28. Manas, D.; Stanek, M.; Manas, M.; Pata, V.; Javorik, J. *Kautschuk Gummi Kunststoffe* 2009, 62, 240.
29. Maya, S.; Mark, R. G. *J Elastom Plast* 2003, 35, 73.
30. Liu, Z. R.; Tand, H. Y. *Handbook of Rubber Industry*; Chemical Industrial Press: Beijing, China, p 557.
31. Coveney, V.; Menger, C. *Wear* 1999, 233, 702.
32. Fukahori, Y.; Liang, H.; Busfield, J. J. C. *Wear* 2008, 265, 387.